PSMD6 as a biomarker for hepatocellular carcinoma: A comprehensive bioinformatics analysis and *in vitro* validation

JIAN LIU[1], TING WANG[2] and ZHENHUA ZHU[3]

[1]Department of Emergency, The First Hospital of Hunan University of Chinese Medicine, Changsha, Hunan 410007, P.R. China; [2]Department of Public Health, The First Hospital of Hunan University of Chinese Medicine, Changsha, Hunan 410007, P.R. China; [3]Otolaryngology-Wide Head and Neck Surgery Department, The First Hospital of Hunan University of Chinese Medicine, Changsha, Hunan 410007, P.R. China

Received February 12, 2025; Accepted February 2, 2026

DOI: 10.3892/mco.2026.2937

Abstract. Hepatocellular carcinoma (HCC) is a lethal malignancy with limited diagnostic biomarkers. The present study aims to comprehensively investigate the expression, clinical prognostic significance, and potential mechanisms of PSMD6 in HCC through comprehensive bioinformatics analyses and *in vitro* experimental validation. *PSMD6* expression in HCC was analyzed using data from the UALCAN, SANGERBOX and TIMER databases. The association between PSMD6 expression and clinicopathological features, patient prognosis, and immune cell filtration was evaluated. Functional enrichment analyses (Gene Ontology and Kyoto Encyclopedia of Genes and Genomes) were performed to identify PSMD6-related signaling pathways, and a protein-protein interaction (PPI) network was constructed using the BioGRID and STRING databases. Key findings from bioinformatics analyses were validated *in vitro* using reverse transcription-quantitative (RT-qPCR) and western blotting in HCC cell lines. *PSMD6* expression was significantly upregulated in HCC compared with adjacent normal tissues (P<0.001), which has been consistently validated by various databases and confirmed by *in vitro* experiments using RT-qPCR and western blotting. High PSMD6 expression was significantly associated with advanced tumor grade and patient age and served as an independent predictor of poor overall survival (P<0.001). In addition, *PSMD6* demonstrated high diagnostic accuracy for HCC (area under the curve=0.877). Moreover, *PSMD6* expression showed a positive correlation with the infiltration levels of $CD4^+$ T cells and B cells in HCC (P<0.05), independent of tumor purity (P>0.05). Functional enrichment analysis indicated that PSMD6 was involved in critical oncogenic pathways, including the cell cycle. PPI network analysis revealed that *PSMD6* interact with several key proteins, such as *PSMC3, PSMD7* and *UCHL5* to achieve a regulatory function in HCC. In conclusion, *PSMD6* is significantly overexpressed in HCC and is strongly associated with tumor progression and poor prognosis. It represents a promising diagnostic biomarker and a potential therapeutic target for HCC.

Correspondence to: Professor Zhenhua Zhu, Otolaryngology-Wide Head and Neck Surgery Department, The First Hospital of Hunan University of Chinese Medicine, 95 Shaoshan Middle Road, Yuhua, Changsha, Hunan 410007, P.R. China
E-mail: zhenhua_787@126.com

Abbreviations: PSMD6, proteasome 26s subunit, non-ATPase 6; LIHC, liver invasive hepatocellular carcinoma; GEO, gene expression omnibus; DAB, diaminobenzidine; ROC, receiver operating characteristic; OS, overall survival; DSS, disease-specific survival; HR, hazard ratio; CI, confidence interval; TNM, tumor-node-metastasis; GO, Gene Ontology; KEGG, Kyoto Encyclopedia of Genes and Genomes

Key words: hepatocellular carcinoma, *PSMD6*, poor prognosis, bioinformatics, *in vitro* analysis

Introduction

Hepatocellular carcinoma (HCC) is the predominant histological subtype of hepatic cancer, comprising 90% of all primary hepatic malignancies worldwide (1). Its high mortality rate and poor prognosis render it a significant global public health threat. In particular, the survival rate of patients with HCC remains among the lowest across all cancer types, with studies indicating a five-year survival rate of only 21%. The prevalence of HCC exhibits notable geographic variation, with China bearing a substantial proportion of the global burden, accounting for more than 50% of all cases globally (2).

A major challenge in managing HCC is that the disease often remains asymptomatic during its early phases, leading to delayed diagnosis (3). As a result, most patients are diagnosed at intermediate or advanced stages, missing the optimal window for curative interventions such as surgical resection, liver transplantation, or percutaneous ablation for early-stage liver cancer (4). Although liver transplantation is considered the most effective treatment for eligible patients, its utility is often limited by high rates of recurrence and metastasis (5-7). Therefore, developing strategies for early precision diagnosis and targeted therapy is critically important. In this end, there is an urgent need to identify effective biomarkers to aid in early screening, accurate diagnosis, treatment evaluation and prognosis prediction for patients with HCC (8).

The pathogenesis of HCC involves dysregulation of key cellular processes such as cell cycle control, apoptosis and DNA repair (9). Among the key molecular drivers is the ubiquitin-proteasome system (UPS), the primary pathway for intracellular protein degradation. The UPS also plays a critical role in regulating antigen processing, signal transduction, and cell cycle progression (10). In HCC, aberrant UPS function, often marked by the overexpression of specific proteasome subunits, has been recognized as a hallmark of HCC, supported by the clinical efficacy of proteasome inhibitors in certain patient subgroups (11).

As cancer cells exhibit rapid proliferation, they generate an increased load of misfolded and damaged proteins, creating a highly promiscuous cellular environment (12), where proteasomes can combine with highly promiscuous substrates selectively and induce the degradation of proteins modified with ubiquitin chains (13). The 26S proteasome selectively recognizes and degrades ubiquitin-tagged proteins, thereby maintaining protein homeostasis. This complex includes PSMD (proteasome 26S subunit, non-ATPase) proteins, which comprise 14 distinct subunits responsible for the recognition and degradation of damaged, misfolded, or foreign proteins (14).

Increasing evidence suggests that several *PSMD* components are overexpressed in various malignancies and may serve as potential biomarkers and therapeutic targets in HCC due to their distinct molecular functions (15,16). For example, *PSMD11* has been reported to promote HCC progression through interactions with *ATP7A*, *DLAT* and *PDHA1 (*17). Similarly, high expression of *PSMD13* is associated with sustained tumor cell activity, epithelial-mesenchymal transition (EMT) and genomic instability (18). However, the roles of numerous other *PSMD* family members in hepatocarcinogenesis remain poorly understood. Notably, 26S proteasome non-ATPase regulatory subunit 6 (*PSMD6*, also known as *Rpn7*) has been implicated in maintaining genomic stability; its knockdown has been shown to induce DNA damage and apoptosis in experimental models (19). Nevertheless, the relationship between *PSMD6* and HCC pathogenesis has not been systematically investigated.

The present study aims to comprehensively analyze the expression patterns of *PSMD6* in HCC at both mRNA and protein levels and to evaluate its potential as a biomarker for early diagnosis and prognosis assessment. Through a combination of bioinformatics analysis and experimental validation, it was aimed to clarify the clinical significance of *PSMD6* and its underlying mechanisms in HCC progression.

Materials and methods

Data acquisition and processing. Transcriptome data (RNA-seq) and corresponding clinical information of the Liver Hepatocellular Carcinoma (LIHC) project were downloaded from The Cancer Genome Atlas (TCGA) portal (https://portal.gdc.cancer.gov).

The initial dataset comprised 424 clinical samples, including 371 tumor tissues and 53 paired adjacent normal tissues. Samples with incomplete clinical information were excluded from subsequent survival and clinical correlation analyses. To augment the normal liver tissue sample size, transcriptome data from 110 normal liver samples were obtained from the Genotype-Tissue Expression (GTEx) project database (https://commonfund.nih.gov/GTEx). All gene expression data were normalized to Transcripts Per Million (TPM) format. For downstream analyses, the TPM values were transformed using log2(TPM + 1) to approximate a normal distribution. All data processing was performed using R software (version 4.2.1; https://www.R-project.org).

Open databases and bioinformatics analysis

Xiantao Toolbox. The Xiantao Toolbox (https://xiantaozi.com/) platform provides a non-coding suite of tools for multi-dimensional bioinformatics analysis without requiring programming expertise. It was utilized in the present study for initial data exploration and specific analytical modules.

TISCH database. Tumor Immune Single-cell Hub (TISCH, http://tisch.comp-genomics.org/) is a curated database dedicated to the tumor microenvironment (TME), providing single-cell RNA sequencing (scRNA-seq) data across various cancer types. It was consulted to explore the cellular composition of the TME in HCC at a single-cell resolution.

BioGRID database. Biological General Repository for Interaction Datasets (BioGRID, https://thebiogrid.org) is a publicly accessible repository of protein, genetic and chemical interactions. This database provides over 2.8 million protein types and genetic interactions, and more than 30.000 chemical interactions, and this database was queried to identify known and predicted protein-protein interactions (PPIs) involving PSMD6.

UALCAN database. UALCAN is a comprehensive web-based bioinformatics toolbox platform (https://ualcan.path.uab.edu/) for analyzing cancer OMICS data, particularly from TCGA. It enables in-depth gene expression analysis, patient survival analysis, and promoter methylation profiling across different tumor subgroups. This database was used to validate *PSMD6* expression patterns and assess its correlation with key clinical parameters (for example, cancer stage and tumor grade).

SANGERBOX database. SANGERBOX is an integrated bioinformatics analysis platform (http://vip.sangerbox.com) offering a user-friendly interface for various analyses, including differential expression, pathway enrichment and Weighted Gene Co-expression Network Analysis (WGCNA). It was employed for specific functional enrichment analyses.

Kaplan-Meier Plotter. Kaplan-Meier Plotter data repository (https://kmplot.com/analysis/) is designed to assess the effect of gene expression on survival outcomes across multiple cancer types using data from sources such as GEO and TCGA. It was used specifically to evaluate the prognostic significance of PSMD6 expression in terms of overall survival (OS) and disease-specific survival (DSS) in the TCGA-LIHC cohort. The platform employs a Cox proportional hazards model, and hazard ratios with 95% confidence intervals and log-rank P-values are reported.

STRING database. STRING is a database of known and predicted PPIs (https://string-db.org). It was used to construct a PPI network centered on PSMD6, with a confidence score threshold set to ensure high-quality interactions.

TIMER database. TIMER (https://cistrome.shinyapps.io/timer/) is a web server for comprehensive analysis of immune cell infiltrates across diverse cancer types using TCGA data. It was utilized to investigate the correlations between PSMD6 expression levels and the abundance of six immune cell populations (B cells, $CD4^+$ T cells, $CD8^+$ T cells,

Table I. Primer sequences.

Gene name	Primer sequence (5'-3')
GAPDH	F: CATCATCCCTGCCTCTACTGG
	R: GTGGGTGTCGCTGTTGAAGTC
Proteasome 26s subunit, non-ATPase 6	F: AAGAACCCCGACTTGCGTATC
	R: GGCTTCATAGTAAGGAGCCATGT

F, forward; R, reverse.

neutrophils, macrophages and dendritic cells) within the HCC TME, with adjustment for tumor purity.

Cell culture. The human immortalized hepatic epithelial cell line (THLE-2) and three human liver cancer cell lines were procured from Zhejiang Meisen Cell Technology Co., Ltd. (THLE-2, cat. no. CTCC-004-0030; HepG2, cat. no. CTCC-DZ-0057; MHCC97-L, cat. no. CTCC-400-0194; MHCC97-H, cat. no. CTCC-0395-Luc1). The 4 cell lines was authenticated using short tandem repeat profiling. The obtained STR profile was compared with reference databases (DSMZ) to confirm identity. Cells were routinely tested for mycoplasma contamination and used within 20 passages after thawing. All cell lines were cultured in RPMI-1640 medium (Gibco; Thermo Fisher Scientific, Inc.), supplemented with 10% heat-inactivated fetal bovine serum (FBS; Gibco; Thermo Fisher Scientific, Inc.) and 1% penicillin-streptomycin (Gibco; Thermo Fisher Scientific, Inc.). Cells were maintained in a humidified incubator at 37˚C with 5% CO_2. Regular mycoplasma testing was performed to ensure cell line authenticity and absence of contamination.

Western blot analysis. Total protein was extracted from cultured cells using RIPA lysis buffer (Guangzhou Biolight Biotechnology Co., Ltd.) containing protease and phosphatase inhibitors (Tiandz, Inc.). Protein concentration was determined using a bicinchoninic acid (BCA) assay kit. Equal amounts of protein (typically 20-30 μg per lane) were separated by 10% SDS-polyacrylamide gel electrophoresis and subsequently transferred onto polyvinylidene difluoride membranes (Seebio; https://www.seebio.cn/). After blocking with 5% (w/v) bovine serum albumin (cat. no. BS114; Biosharp Life Sciences) in Tris-buffered saline with 0.1% Tween-20 (TBST) for 1 h at room temperature, the membranes were incubated overnight at 4˚C with the primary antibody against PSMD6 (1:1,000; cat. no. Ag3251; Proteintech Group, Inc.) and GAPDH as a loading control (1:50,000; cat. no. 60004-1-Ig; Proteintech Group, Inc.). Following three washes with TBST, the membranes were incubated with an appropriate horseradish peroxidase (HRP)-conjugated secondary antibody (1:50,000; cat. no. BL003A; Biosharp Life Sciences) for 1 h at room temperature. Protein bands were visualized using an enhanced chemiluminescence (ECL) detection kit (MilliporeSigma) and imaged with a chemiluminescence imaging system. Densitometric analysis of the bands was performed using ImageJ software (version 1.8.0.; National Institutes of Health). All experiments were independently repeated at least three times.

Reverse transcription-quantitative PCR (RT-qPCR). Total RNA was extracted from cultured cells using TriQuick Reagent (Beijing Solarbio Science & Technology Co., Ltd.) according to the manufacturer's instructions. RNA concentration and purity (A260/A280 ≥1.8) were measured using a NanoDrop spectrophotometer (Thermo Fisher Scientific, Inc.). Complementary DNA (cDNA) was synthesized from 1 μg of total RNA using a 5X RT SuperMix for qPCR kit (Vazyme Biotech Co., Ltd.). qPCR was performed using a 2X SYBR Green qPCR Master Mix (Vazyme Biotech Co., Ltd.) on an iQ5 Multicolor Real-Time PCR Detection System (Bio-Rad Laboratories, Inc.). The PCR cycling conditions were as follows: Initial denaturation at 95˚C for 30 sec, followed by 40 cycles of 95˚C for 5 sec and 60˚C for 30 sec. The relative mRNA expression level of PSMD6 was calculated using the $2^{-\Delta\Delta Cq}$ method (20), with GAPDH as the internal reference gene. The specific primer sequences used are listed in Table I. Each experiment was performed in triplicate wells and repeated independently three times.

Statistical analysis. Bioinformatics data analysis was primarily conducted using R software (version 4.2.1 or 3.6.4 as specified for specific packages). Differential expression of PSMD6 between HCC tumors and normal tissues was assessed using the Wilcoxon rank-sum test. Correlations between PSMD6 expression and immune cell infiltration levels were evaluated using Pearson's or Spearman's correlation coefficients via the corr.test function in the Psych R package (v2.1.6; CRAN.R-project.org/package=psych). Survival analysis was performed using the Kaplan-Meier method, and differences in survival curves were compared using the log-rank test via the Survival R package. For *in vitro* experiments, data are presented as the mean ± standard deviation ($\bar{x}\pm s$) from at least three independent experiments. Statistical comparisons between two groups were analyzed using independent two-tailed unpaired Student's t-test. Comparisons among multiple groups were performed using one-way analysis of variance (ANOVA) followed by Dunnett's multiple comparison test. $P<0.05$ was considered to indicate a statistically significant difference.

Results

PSMD6 is significantly overexpressed in HCC and correlates with adverse clinicopathological features. Investigation was initiated by assessing the pan-cancer expression profile of PSMD6 to determine its potential relevance in oncogenesis. To tackle this, the pan-cancer expression of *PSMD6* was assessed

Table II. Comparison of proteasome 26s subunit, non-ATPase 6 expression in multiple tumor and non-tumor tissues.

Cancer	Tumor	Normal	P-value	Result
GBM	6.11±0.42	4.86±1.30	$4.7x10^{-72}$	Increase
GBMLGG	5.89±0.35	4.86±1.30	$1.1x10^{-187}$	Increase
LGG	5.83±0.30	4.86±1.30	$4.5x10^{-150}$	Increase
UCEC	5.85±0.56	5.64±0.27	$2.1x10^{-3}$	Increase
BRCA	5.96±0.47	5.77±0.23	$1.2x10^{-16}$	Increase
COAD	5.77±0.42	5.36±1.70	$4.4x10^{-13}$	Increase
COADREAD	5.80±0.42	5.37±1.68	$2.2x10^{-18}$	Increase
PRAD	5.73±0.42	5.60±0.35	$1.5x10^{-4}$	Increase
STAD	5.37±0.46	4.99±1.56	$6.0x10^{-8}$	Increase
LIHC	5.21±0.46	4.79±0.46	$3.6x10^{-20}$	Increase
WT	6.32±0.46	5.65±1.35	$3.2x10^{-21}$	Increase
READ	5.92±0.39	5.68±0.26	0.04	Increase
ALL	5.83±0.76	4.00±1.34	$1.8x10^{-39}$	Increase
LAML	6.08±0.42	4.00±1.34	$5.6x10^{-64}$	Increase
CHOL	5.06±0.44	4.56±0.21	$2.8x10^{-4}$	Increase
LUAD	5.53±0.41	5.76±0.87	$1.7x10^{-30}$	Decrease
ESCA	5.62±0.40	5.71±1.27	$3.0x10^{-13}$	Decrease
STES	5.45±0.46	5.53±1.38	$1.1x10^{-22}$	Decrease
KIRP	5.50±0.52	5.65±1.35	$6.7x10^{-10}$	Decrease
KIPAN	5.31±0.51	5.65±1.35	$1.8x10^{-28}$	Decrease
KIRC	5.18±0.46	5.65±1.35	$2.5x10^{-39}$	Decrease
LUSC	5.59±0.40	5.76±0.87	$1.2x10^{-20}$	Decrease
THCA	5.63±0.32	5.71±0.90	$2.4x10^{-8}$	Decrease
OV	5.36±0.91	5.58±0.29	$3.2x10^{-4}$	Decrease
PAAD	5.50±0.36	6.48±1.90	$4.6x10^{-44}$	Decrease
TGCT	6.34±0.52	7.22±0.48	$6.1x10^{-34}$	Decrease
UCS	5.76±0.69	5.95±0.24	$2.7x10^{-3}$	Decrease
PCPG	5.59±0.53	6.20±0.43	0.05	Decrease
ACC	5.80±0.69	5.93±1.47	0.01	Decrease
KICH	5.49±0.57	5.65±1.35	$2.8x10^{-4}$	Decrease

GBM, glioblastoma multiforme; LGG, brain lower grade glioma; UCEC, uterine corpus endometrial carcinoma; BRCA, breast invasive carcinoma; COAD, colon adenocarcinoma; PRAD, prostate adenocarcinoma; STAD, stomach adenocarcinoma; LIHC, liver hepatocellular carcinoma; WT, Wilms tumor; READ, rectum adenocarcinoma; ALL, acute lymphoblastic leukemia; LAML, acute myeloid leukemia; CHOL, cholangiocarcinoma; LUAD, lung adenocarcinoma; ESCA, esophageal carcinoma; STES, stomach and esophageal cancer; KIRP, kidney renal papillary cell carcinoma; KIRC, kidney renal clear cell carcinoma; LUSC, lung squamous cell carcinoma; THCA, thyroid carcinoma; OV, ovarian serous cystadenocarcinoma; PAAD, pancreatic adenocarcinoma; TGCT, testicular germ cell tumors; UCS, uterine carcinosarcoma; PCPG, pheochromocytoma and paraganglioma; ACC, adrenocortical carcinoma; KICH, kidney chromophobe.

utilizing SANGERBOX database, and it was revealed that *PSMD6* was significantly dysregulated across multiple cancer types, being upregulated in 15 and downregulated in 15 other malignancies (Table II, Fig. 1A). Consistent findings were gained through analyzing with UALCAN data repository (Fig. 1B). This pan-cancer aberration highlighted PSMD6 as a gene of general interest in cancer research.

Subsequent focused analysis on LIHC from the TCGA cohort demonstrated a pronounced overexpression of PSMD6 in tumor specimens (n=371) compared with adjacent normal tissues (n=50; P<0.001; Fig. 2A and B).

To evaluate the clinical relevance of PSMD6 overexpression, its correlation with key clinicopathological parameters was examined using Xiantao tools. PSMD6 levels were significantly elevated in HCC tissues across all pathology grades (G1-G4), T stages (T1-T4), nodal involvement (N0/N1), metastasis status (M0/M1), as well as irrespective of patient weight, sex and ethnicity (all P<0.05) (Fig. 3A-G). This consistent upregulation across diverse clinical subgroups underscores the potential of PSMD6 as a robust biomarker associated with HCC progression and aggressiveness.

High PSMD6 expression predicts poor prognosis in patients with HCC. Given the strong association of PSMD6 with advanced disease stages, the prognostic value of PSMD6 expression in HCC was next evaluated. A 5-year survival analysis was conducted on patients using the UALCAN database, and the results showed that patients with high PSMD6

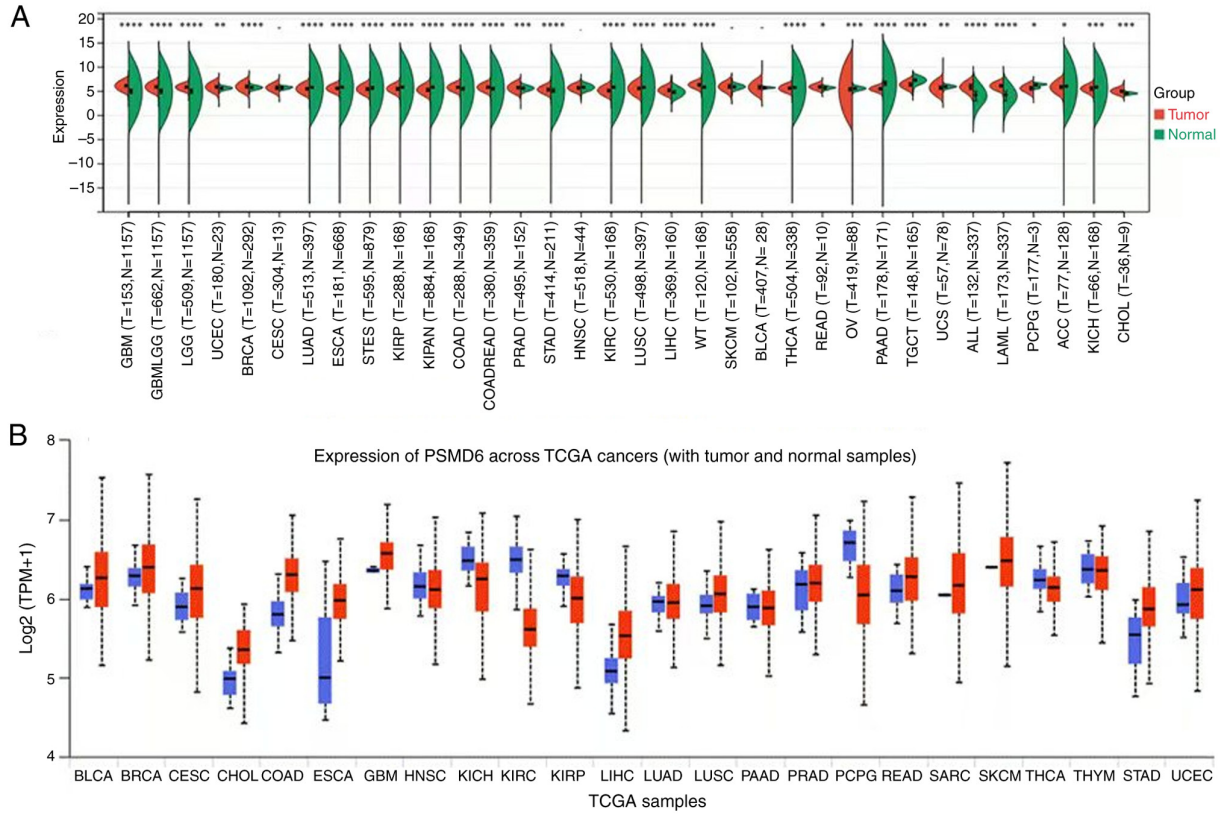

Figure 1. Pan-cancer analysis of PSMD6 expression. (A) PSMD6 mRNA expression levels across various cancer types from the TCGA project, as analyzed via the SANGERBOX database. (B) Validation of PSMD6 expression in multiple cancers using the UALCAN database. Data are presented as log2-transformed TPM values. PSMD6 is significantly upregulated in LIHC compared with normal tissue *P<0.05, **P<0.01, ***P<0.001 and ****P<0.0001. PSMD6, proteasome 26s subunit, non-ATPase 6; TCGA, The Cancer Genome Atlas; TPM, transcripts per million; LIHC, liver hepatocellular carcinoma.

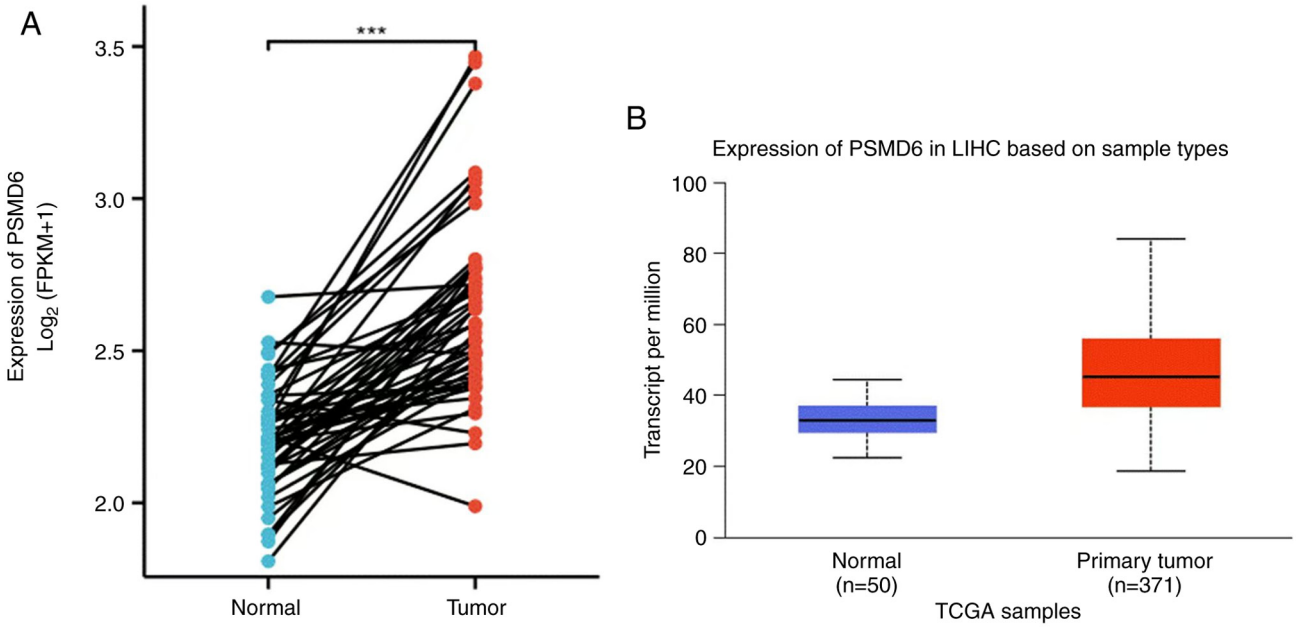

Figure 2. Differential expression of PSMD6 in LIHC. (A and B) PSMD6 expression is significantly higher in LIHC tumor tissues (n=371) compared with (A) adjacent normal tissues (n=50) from TCGA or (B) combined normal tissues from TCGA and GTEx (n=163), as analyzed by XIANTAO tools and UALCAN, respectively. ***P<0.001. PSMD6, proteasome 26s subunit, non-ATPase 6; LIHC, liver hepatocellular carcinoma; TCGA, The Cancer Genome Atlas.

expression (n=90) had a significantly lower probability of overall survival compared with those with low expression (n=275; P<0.05; Fig. 4A).

In the subgroup analysis stratified by pathology grade, the best prognosis was found in grade 1 patients with a low expression level of *PSMD6*, and the worst prognosis was found in grade

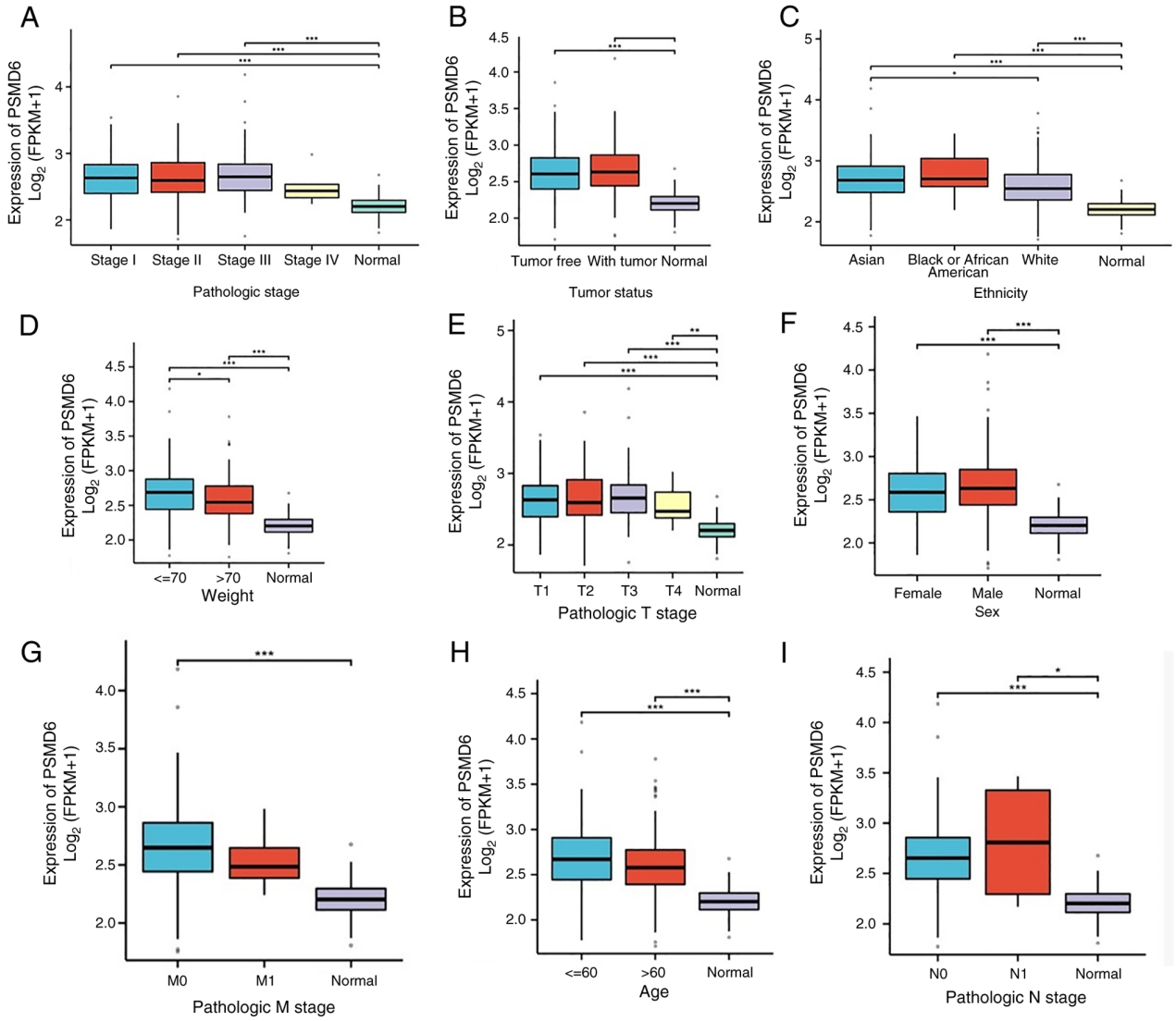

Figure 3. Association between PSMD6 expression and clinicopathological characteristics in LIHC. (A-I) Box plots showing PSMD6 expression levels stratified by (A) pathologic stage, (B) tumor status, (C) ethnicity, (D) patient weight, (E) pathologic T stage, (F) sex, (G) pathologic M stage, (H) age and (I) pathologic N stage. Analyses were performed using data from The Cancer Genome Atlas-LIHC cohort via XIANTAO tools. *P<0.05, **P<0.01 and ***P<0.001. PSMD6, proteasome 26s subunit, non-ATPase 6; LIHC, liver hepatocellular carcinoma.

4 patients highly expressing *PSMD6*. In the subgroup analysis stratified by ethnicity, African Americans with high *PSMD6* expression had the worst prognosis, while Caucasians with low *PSMD6* expression had the best prognosis. In the subgroup analysis stratified by sex, female group with high expression of *PSMD6* had the most unfavorable prognosis, and female group with low expression of *PSMD6* had the best prognosis. All comparisons exhibited statistical significance (Fig. 4B-D).

Further validation using the SANGERBOX database corroborated these findings across multiple survival endpoints. High PSMD6 expression was significantly associated with poorer OS, DSS, disease-free interval and progression-free interval (all P<0.05; Fig. 5).

The robustness of PSMD6 as a prognostic indicator was confirmed by Receiver Operating Characteristic (ROC) curve analysis utilizing the Kaplan-Meier Plotter data repository. Cases were classified into high-expression groups and low-expression groups relying on the mean expression at different quantiles. The analysis revealed that *PSMD6* gene expression had a favorable prognostic value (P=0.00039; Fig. 6A), which yielded an area under the curve of 0.877 (95% confidence interval: 0.837-0.916; Fig. 6B), indicating high diagnostic accuracy.

Experimental validation confirms elevated PSMD6 expression in HCC cell lines. To further validate bioinformatic predictions, *in vitro* experiments were performed using a normal human hepatic cell line (THLE-2) and three distinct HCC cell lines (HepG2, MHCC97-L and MHCC97-H). RT-qPCR analysis demonstrated that *PSMD6* mRNA levels were significantly elevated in all three HCC cell lines compared with the normal hepatic cell line (P<0.0001; Fig. 7).

This transcriptional upregulation was further confirmed at the protein level by western blot analysis, which revealed consistently higher PSMD6 protein expression in the HCC cell lines (Fig. 8). These findings from mRNA and protein levels provide strong evidence for the overexpression of PSMD6 in HCC.

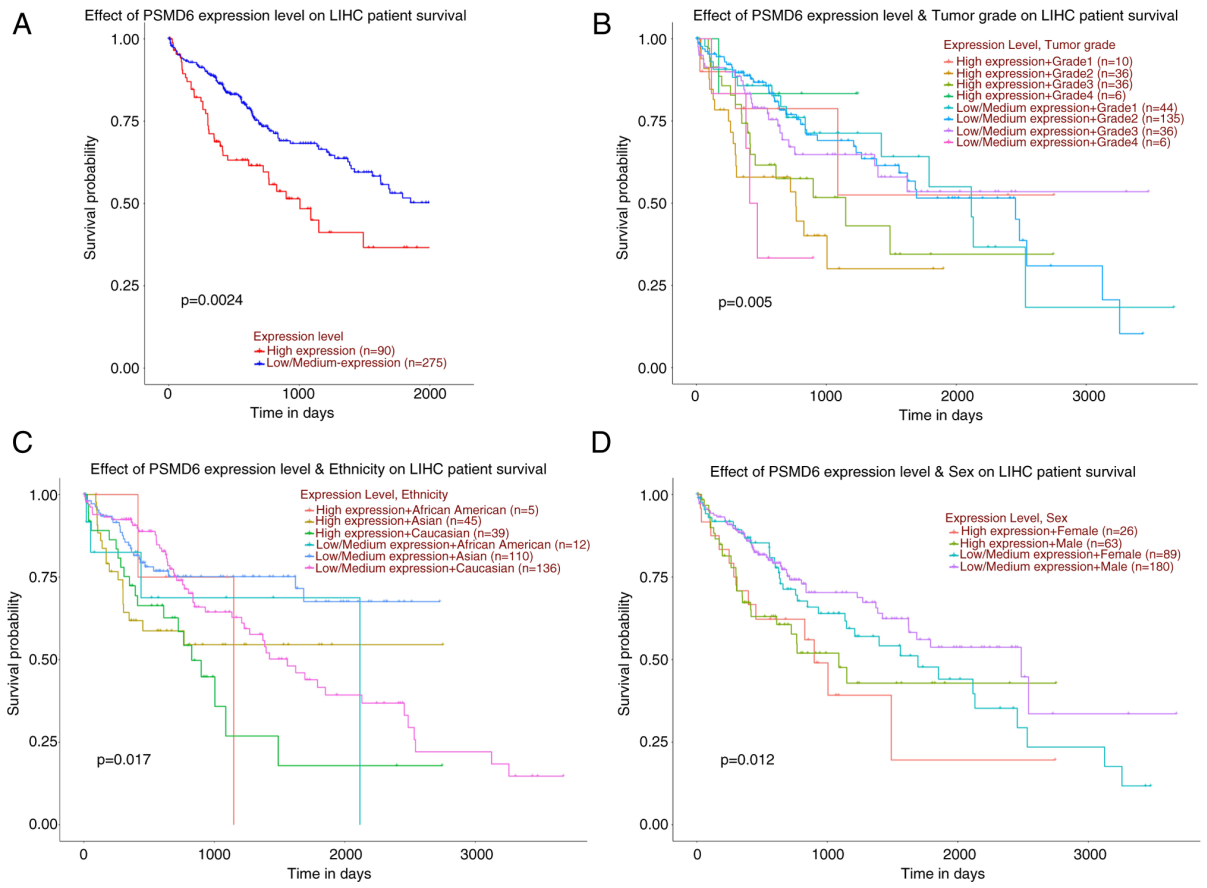

Figure 4. Survival analysis of PSMD6 in LIHC using UALCAN. Kaplan-Meier curves showing the impact of PSMD6 expression on patient survival. (A) OS of all patients with LIHC stratified by high and low PSMD6 expression. (B-D) Subgroup analysis of OS based on (B) tumor grade, (C) ethnicity and (D) sex. PSMD6, proteasome 26s subunit, non-ATPase 6; LIHC, liver hepatocellular carcinoma; OS, overall survival.

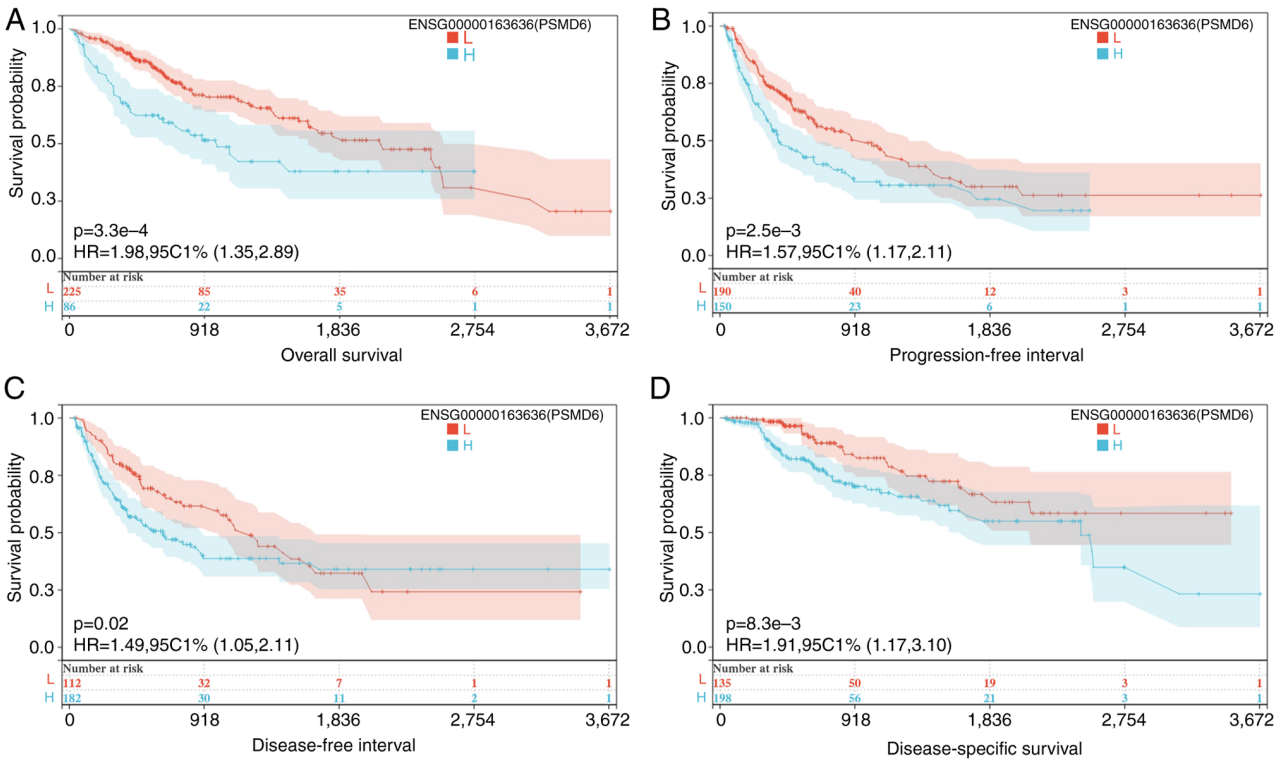

Figure 5. Prognostic value of PSMD6 in LIHC using SANGERBOX. (A-D) Kaplan-Meier survival analysis demonstrating the relationship between PSMD6 expression and (A) overall survival, (B) progression-free interval, (C) disease-free interval, and (D) disease-specific survival. PSMD6, proteasome 26s subunit, non-ATPase 6; HR, hazard ratio.

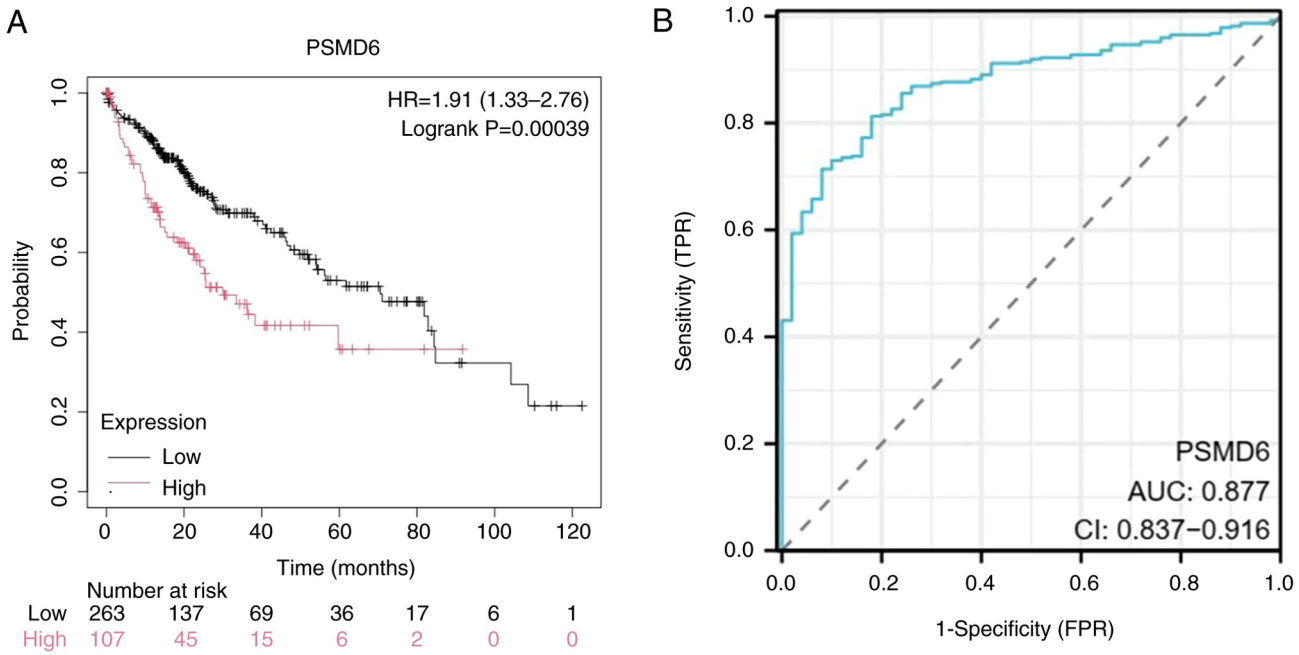

Figure 6. Diagnostic and prognostic value of PSMD6. (A) Kaplan-Meier plot from the Kaplan-Meier Plotter database confirms that high PSMD6 expression predicts poor overall survival in patients with LIHC. (B) Receiver operating characteristic curve analysis (via XIANTAO tools) evaluating the diagnostic power of PSMD6 to distinguish LIHC tumors from normal tissues (FDR=1%). PSMD6, proteasome 26s subunit, non-ATPase 6; LIHC, liver hepatocellular carcinoma; AUC, area under the curve; HR, hazard ratio; CI, confidence interval.

PSMD6 expression correlates with immune cell infiltration in the TME. Tumorigenesis and development usually correlate to infiltration of immune cells including B cell and macrophage. In this context, the TIMER database was utilized to investigate the relationship between *PSMD6* expression and the abundance of various immune cell populations within the HCC TME. *PSMD6* expression was found to be independent of tumor purity (r=0.007, P=0.89). However, it exhibited significant positive correlations with the infiltration levels of B cells (r=0.191, P=0.00003), $CD8^+$ T cells (r=0.1416, P=0.0087), $CD4^+$ T cells (r=0.2287, P=1.84x10^{-5}), neutrophils (r=0.299, P=1.48x10^{-8}), macrophages (r=0.307, P=6.9x10^{-9}) and dendritic cells (r=0.268, P=5.45x10^{-7}) (Table III, Fig. 9A).

To gain deeper, single-cell resolution insights, the TISCH database was used to analyze the enrichment of *PSMD6* gene in tumor and its immune microenvironment at the single-cell level. Analysis of the GSE140228_SmartSeq2 and GSE98638 datasets revealed that *PSMD6* is predominantly enriched within specific immune cell subsets, including monocytes/macrophages (mono/macro) and natural killer (NK) cells in GSE140228_ smartseq2 single-cell cohort, and in conventional $CD4^+$ T cells (cd4tconv) and $CD8^+$ T cells in GSE 98638 single-cell cohort (Fig. 9B-D). This pattern suggests that PSMD6 may influence the immune contexture of HCC, potentially contributing to the immunosuppressive microenvironment often observed in advanced tumors.

Functional enrichment and protein interaction networks implicate PSMD6 in key oncogenic processes. To elucidate the potential biological functions and pathways through which PSMD6 contributes to hepatocarcinogenesis, comprehensive functional enrichment analysis was performed. Currently, Gene Ontology (GO) functional and Kyoto Encyclopedia of Genes and Genomes (KEGG) pathway enrichment evaluations are the methods that are used most frequently.

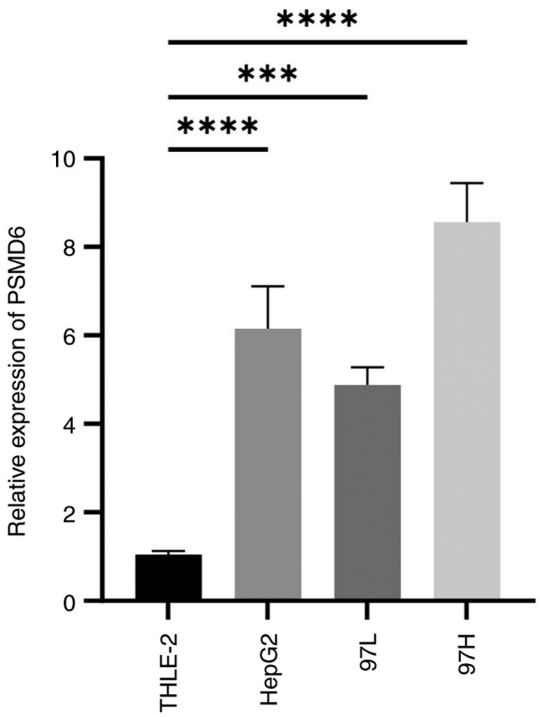

Figure 7. Validation of PSMD6 mRNA expression in cell lines. Relative mRNA expression levels of PSMD6 in a normal human hepatocyte cell line (THLE-2) and three hepatocellular carcinoma cell lines (HepG2, MHCC97-L and MHCC97-H) as determined by reverse transcription-quantitative PCR. Data are presented as the mean ± SD. ***P<0.001 and ****P<0.0001. PSMD6, proteasome 26s subunit, non-ATPase 6.

Table III. Relationship between proteasome 26s subunit, non-ATPase 6 and immune cells in LIHC.

Cancer type	Variable	partial.cor	P-value
LIHC	Purity	0.007451	0.890161
LIHC	B cell	0.191259	0.000361
LIHC	$CD8^+$ T cell	0.141669	0.008701
LIHC	$CD4^+$ T cell	0.2287	$1.84x10^{-5}$
LIHC	Macrophage	0.307234	$6.90x10^{-9}$
LIHC	Neutrophil	0.299014	$1.48x10^{-8}$
LIHC	Dendritic cell	0.267707	$5.45x10^{-7}$

LIHC, liver hepatocellular carcinoma.

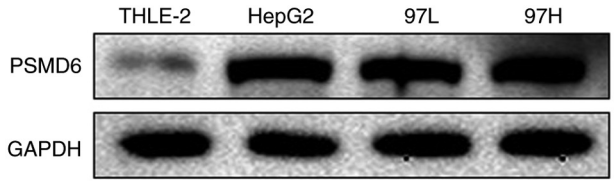

Figure 8. Validation of PSMD6 protein expression in cell lines. Western blot analysis confirming the elevated protein expression of PSMD6 in hepatocellular carcinoma cell lines (HepG2, MHCC97-L and MHCC97-H) compared with the normal hepatocyte cell line THLE-2. GAPDH was used as a loading control. PSMD6, proteasome 26s subunit, non-ATPase 6.

KEGG pathway analysis indicated that PSMD6-coexpressed genes were significantly enriched in crucial cancer-related pathways, including RNA transmit, Ubiquitin mediated proteolysis, Cell cycle, mRNA surveillance pathway, Spliceosome, Herpes simplex virus 1 infection, basal transcription factors, shigellosis, endocytosis and DNA replication (Fig. 10). Concurrently, GO functional analysis highlighted terms such as nucleoplasm, chromosome organization, protein-containing complex and catalytic complex (Fig. 10). The consistent emergence of cell cycle and protein degradation pathways aligns with the known role of the 26S proteasome, of which *PSMD6* is a regulatory subunit in controlling cell cycle progression and protein turnover.

Furthermore, a PPI network was constructed to identify potential functional partners of PSMD6. Queries using the BioGRID and STRING databases revealed that PSMD6 interacts with several core proteasomal subunits, including PSMC3, PSMD7, UCHL5, PSMA2 and PSMB7 ($P<0.001$, Fig. 11).

Moreover, as a PPI network can facilitate an improved understanding of intracellular protein functions and signal delivery, a PSMD6-centered PPI network was constructed using STRING database. Multiple PSMD6-interacting proteins were identified, such as PSMC1, PSMA2, PSMA4 and PSMB7 (Fig. 12), suggesting that its oncogenic effects may be mediated through the regulation of proteasome activity and subsequent impacts on critical cellular processes.

Discussion

Primary findings. The present multi-faceted analysis demonstrates that PSMD6 is significantly overexpressed in HCC and is strongly associated with malignant progression and poor patient survival. Its influence likely extends to shaping the tumor immune microenvironment. These findings nominate PSMD6 as a promising diagnostic biomarker and a potential therapeutic target worthy of further investigation in HCC.

Clinical significance and oncogenic role of PSMD6 in HCC. Primary liver cancer is the seventh-most frequently occurring cancer in the world and the second-most common cause of cancer mortality (21). China has the greatest number of primary liver cases, attributable to both an elevated rate (18.3 per 100,000) and the world's largest population (1.4 billion persons) (22). Specifically, HCC is the dominant type of liver cancer, accounting for ~75% of all liver cancers (23).

With the development of surgical intervention, chemotherapy, targeted treatment and immunotherapy, the survival rate of HCC cases has benefited more from multidisciplinary treatment approaches. However, the survival rate remains low, highlighting a pretty grim situation (24). Therefore, HCC remains a formidable global health challenge, characterized by high mortality and limited therapeutic options for advanced-stage patient.

The quest for reliable biomarkers for early detection and prognosis prediction is therefore paramount. To identify HCC early, current screening and surveillance strategies depend on reliable and convenient serum biomarkers, but only alpha-fetoprotein (AFP) has been extensively applied in clinical settings (25). However, AFP has poor sensitivity and specificity. The present study identified PSMD6 as a potential key player in HCC pathogenesis. Bioinformatics analysis across multiple databases (for example, TCGA and GTEx) consistently revealed significant upregulation of PSMD6 in HCC tissues compared with normal liver tissues. This finding was robustly validated *in vitro*, where both mRNA and protein levels of PSMD6 were markedly elevated in HCC cell lines (HepG2, MHCC97-L, MHCC97-H) compared with the normal hepatic THLE-2 cell line.

These findings align with and extend previous bioinformatics studies that also identified PSMD6 as a differentially methylated gene with significant prognostic value in HCC (26,27). The consistency of PSMD6 overexpression across diverse cohorts and its strong association with clinical outcomes underscore its potential as a robust diagnostic and prognostic biomarker.

Potential mechanisms underlying PSMD6 in HCC. Proteasomes rapidly catalyze a diverse range of biological reactions and then regulate the bioactivity of multiple cells (28). In a previous study, a proteasome system in *Caenorhabditis elegans* germline was constructed and it was found that *PSMD6* downregulation led to reduced proteasome proteolytic activity and cell cycle defect (29). *PSMD* family members may exhibit an increasing trend in tumors due to the characteristics of extremely high protein metabolic level and very short cell division cycle in tumor cells. The PPI network analysis revealed that PSMD6 interacts with core proteasomal subunits (for example, PSMC3, PSMD7 and PSMA2), underscoring its integral role within the 26S proteasome complex. This interaction network suggests that the oncogenic effects of PSMD6 are likely mediated through the regulation of proteasome activity, impacting a wide array of downstream cellular processes.

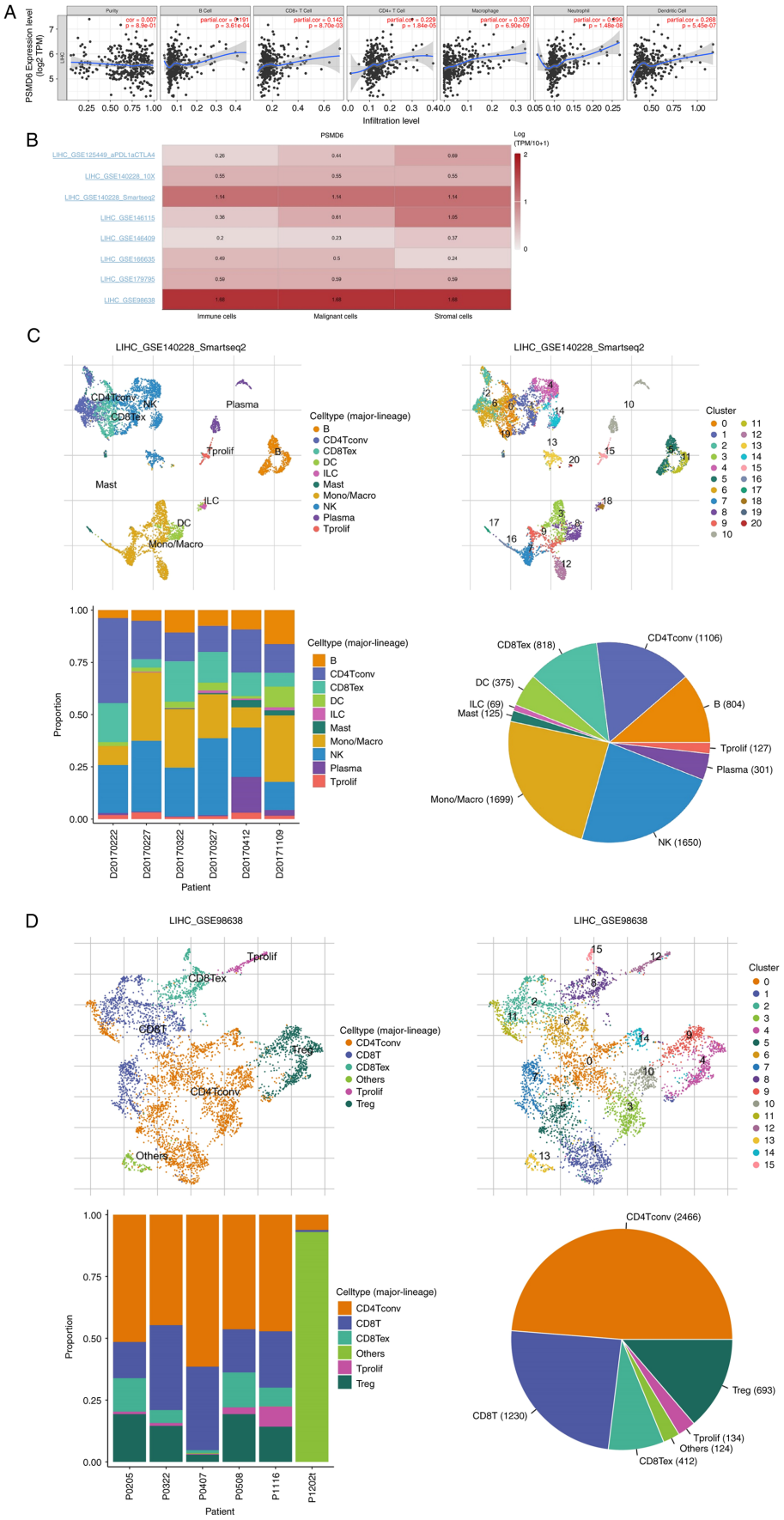

Figure 9. Correlation between PSMD6 expression and immune cell infiltration in the LIHC tumor microenvironment. (A) Scatter plots showing the correlation between PSMD6 expression (log2 TPM) and the abundance of various immune cell types, estimated by the TIMER2.0 algorithm. Statistical significance was determined by Spearman's correlation. (B) Overview of the TISCH database analysis showing the immune landscape of LIHC. (C and D) Single-cell RNA-seq analysis from the TISCH database illustrating the distribution and expression levels of PSMD6 (color scale) across immune cell clusters in the (C) GSE140228_Smartseq2 and (D) GSE98638 datasets. PSMD6, proteasome 26s subunit, non-ATPase 6; LIHC, liver hepatocellular carcinoma.

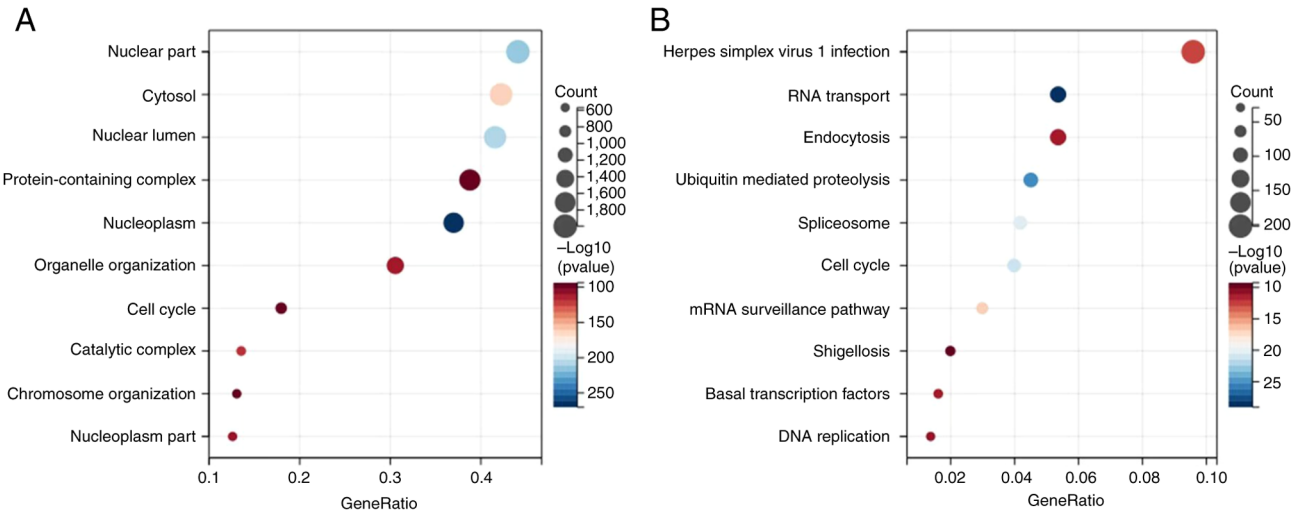

Figure 10. Functional enrichment analysis of PSMD6-coexpressed genes in LIHC. (A) Significantly enriched Kyoto Encyclopedia of Genes and Genomes pathways and (B) Gene Ontology terms (Biological Process, Cellular Component, Molecular Function) for genes correlated with PSMD6 expression in The Cancer Genome Atlas-LIHC cohort. The bubble chart size and color represent the number of genes and the significance level (-log10(P-value)), respectively. PSMD6, proteasome 26s subunit, non-ATPase 6; LIHC, liver hepatocellular carcinoma.

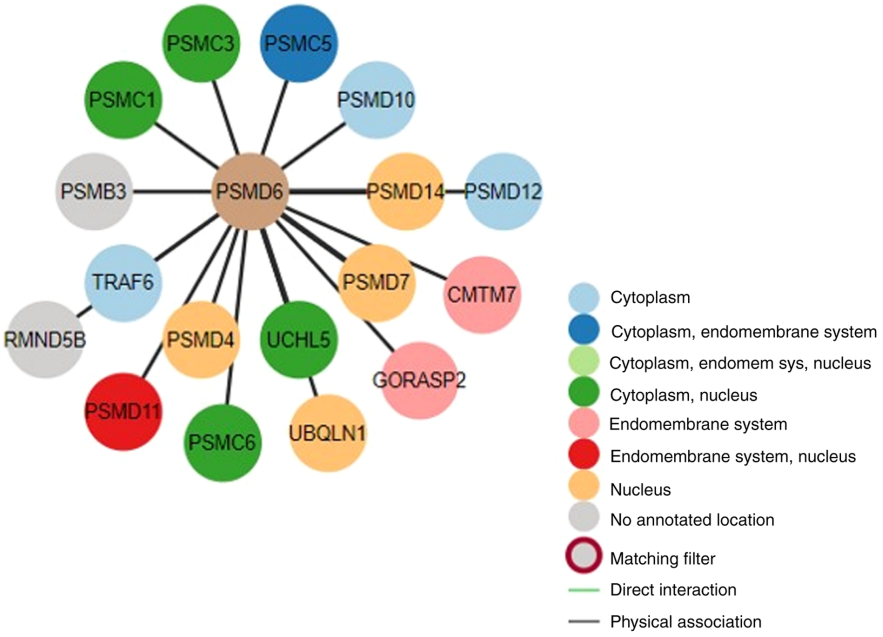

Figure 11. Analysis of the interaction between proteasome 26s subunit, non-ATPase 6 and protein using BioGRID database.

Dysregulation of UPS components, including various PSMD family members, is increasingly recognized as a hallmark of cancer, contributing to uncontrolled proliferation and evasion of apoptosis. The functional enrichment analyses (GO and KEGG) of the present study shed light on the potential mechanisms by which PSMD6 contributes to hepatocarcinogenesis. PSMD6 was significantly enriched in essential biological processes such as the cell cycle, ubiquitin-mediated proteolysis and DNA replication.

A pivotal finding of the present study is the significant correlation between PSMD6 expression and immune cell infiltration. PSMD6 levels positively correlated with the abundance of various immune cells, including B cells, $CD4^+$ T cells, $CD8^+$ T cells, macrophages and dendritic cells. scRNA-seq data from the TISCH database further indicated that PSMD6 is enriched in specific immune subsets including monocytes/macrophages, NK cells and T cells within the HCC microenvironment. This suggests that PSMD6 may influence the functional state of the immune landscape, potentially fostering an immunosuppressive niche that facilitates immune evasion. The role of the immune microenvironment in determining HCC prognosis is well-established, and the current findings position PSMD6 as a novel modulator within this context.

Immunotherapy is important for patients with HCC (30,31). Given the significant connection amid the expression of *PSMD6* and immune cell infiltration, patients with HCC with poor prognosis and survival may benefit from immunotherapy.

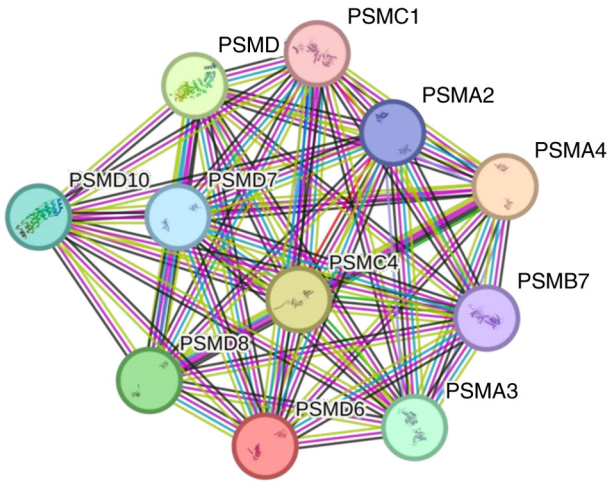

Figure 12. Analyzing the Interaction between proteasome 26s subunit, non-ATPase 6 and proteins in STRING database.

However, whether PSMD6 gene expression affects the effectiveness of immunotherapy warrants further validation.

The present study also noted that Zhou *et al* (27) previously proposed in their research that PSMD6 and its homolog PSMD11 may participate in liver cancer progression and treatment response by regulating proteasome dependent protein degradation pathways, thereby affecting the stability of key cancer proteins such as p53 and Cyclin. This hypothesis provides an important mechanistic perspective for the findings of the present study. The experimental results further support this viewpoint: PSMD6 expression is significantly upregulated in liver cancer tissues, and its high expression is closely related to poor prognosis in patients. Based on previous studies, it was hypothesized that PSMD6 may promote the development of liver cancer through the following pathways: Enhancing proteasome activity and accelerating the degradation of tumor suppressor proteins; regulating the stability of cell cycle and apoptosis related proteins through the ubiquitin proteasome system; synergistic effect with subunits such as PSMD11 affects the proliferation and invasion ability of liver cancer cells. Future research can further validate the specific regulatory mechanism of PSMD6 in liver cancer by knocking down/overexpressing it and detecting downstream target protein levels, providing new ideas for targeted proteasome subunits in liver cancer therapy.

While the integrated bioinformatics and preliminary experimental data highlight the significance of PSMD6 in HCC, the present study has several limitations. First, the bioinformatic findings, though validated across multiple databases, require further confirmation in larger, prospectively collected clinical cohorts to solidify their clinical translatability. Differences in sample sources, sequencing platforms and batches in public databases may lead to biased results, affecting the comparability of *PSMD6* expression. Second, the precise molecular mechanisms by which PSMD6 regulates the cell cycle, immune infiltration and other cancer-related pathways remain to be fully elucidated through detailed functional experiments. Only partial *in vitro* experimental studies were conducted without tissue validation. No stratified analysis was conducted in the present study based on liver cancer subtypes, staging, or treatment response, which may mask potential heterogeneity and therefore lead to weak clinical correlation analysis Although the co-expression network or pathway enrichment of *PSMD6* can be predicted, its upstream regulation (such as methylation, miRNA) and downstream effects in liver cancer still require experimental exploration. Prospective cohorts and animal models are needed to further validate its prognostic value and therapeutic potential.

In conclusion, PSMD6 was found to be significantly overexpressed in HCC and is strongly associated with malignant progression and poor patient survival. Its influence likely extends to shaping the tumor immune microenvironment. These findings nominate *PSMD6* as a promising diagnostic biomarker and a potential therapeutic target worthy of further investigation in HCC. Further experiments and clinical samples are needed for verification.

Acknowledgements

Not applicable.

Funding

No funding was received.

Availability of data and materials

The data generated in the present study may be requested from the corresponding author.

Authors' contributions

JL proposed the initial research concept, was responsible for collecting the data from the database, actively participated in conducting the experiments, and wrote the first complete version of the manuscript. TW contributed to the study design, performed the PCR and Western blot experiments, and critically revised the manuscript for important intellectual content in response to the editor's comments. ZZ contributed to the study design and methodology, provided critical supervision and guidance throughout the experimental phase, rigorously validated all collected data, and meticulously reviewed, critiqued, and revised multiple drafts of the manuscript to ensure its academic rigor and clarity. All authors read and approved the final version of the manuscript. JL and TW confirm the authenticity of all the raw data.

Ethics approval and consent to participate

The present study was conducted in accordance with the declaration of Helsinki and was approved by the Ethics Committee of The First Hospital of Hunan University of Chinese Medicine (approval no. HN-LL-LW-2024-062; Changsha, China).

Patient consent for publication

Not applicable.

Competing interests

The authors declare that they have no competing interests.

References

1. Calderaro J, Seraphin TP, Luedde T and Simon TG: Artificial intelligence for the prevention and clinical management of hepatocellular carcinoma. J Hepatol 76: 1348-1361, 2022.
2. Zheng RS, Chen R, Han BF, Wang SM, Li L, Sun KX, Zeng HM, Wei WW and He J: Cancer incidence and mortality in China, 2022. Zhonghua Zhong Liu Za Zhi (Chinese) 46: 221-231, 2024.
3. Qiu F, Qiu F, Liu L, Liu J, Xu J and Huang X: The role of dermcidin in the diagnosis and staging of hepatocellular carcinoma. Genet Test Mol Biomarkers 22: 218-223, 2018.
4. Urquijo-Ponce JJ, Alventosa-Mateu C, Latorre-Sánchez M, Castelló-Miralles I and Diago M: Present and future of new systemic therapies for early and intermediate stages of hepatocellular carcinoma. World J Gastroenterol 30: 2512-2522, 2024.
5. Hoti E. and Adam R: Liver transplantation for primary and metastatic liver cancers. Transpl Int 21: 1107-1117, 2008.
6. Sapisochin G and Bruix J: Liver transplantation for hepatocellular carcinoma: outcomes and novel surgical approaches. Nat Rev Gastroenterol Hepatol 14: 203-217, 2017.
7. Neuberger J: An update on liver transplantation: A critical review. J Autoimmun 66: 51-59, 2016.
8. Gao S, Gang J, Yu M, Xin G and Tan H: Computational analysis for identification of early diagnostic biomarkers and prognostic biomarkers of liver cancer based on GEO and TCGA databases and studies on pathways and biological functions affecting the survival time of liver cancer. BMC Cancer 21: 791, 2021.
9. Fabregat I: Dysregulation of apoptosis in hepatocellular carcinoma cells. World J Gastroenterol 15: 513-520, 2009.
10. Li X, Li X, Hu Y, Liu O, Wang Y, Li S, Yang Q and Lin B: PSMD8 can serve as potential biomarker and therapeutic target of the PSMD family in ovarian cancer: based on bioinformatics analysis and in vitro validation. BMC Cancer 23: 573, 2023.
11. Jiang L, Qi X, Lai M, Zhou J, Yuan M, You J, Liu Q, Pan J, Zhao L, Ying M, *et al*: WDR20 prevents hepatocellular carcinoma senescence by orchestrating the simultaneous USP12/46-mediated deubiquitination of c-Myc. Proc Natl Acad Sci USA 121: e2407904121, 2024.
12. Wang M, Yu F and Li P: Intratumor microbiota in cancer pathogenesis and immunity: From mechanisms of action to therapeutic opportunities. Front Immunol 14: 1269054, 2023.
13. Li H, Ji Z, Paulo JA, Gygi SP and Rapoport TA: Bidirectional substrate shuttling between the 26S proteasome and the Cdc48 ATPase promotes protein degradation. Mol Cell 84: 1290-1303. e7, 2024.
14. Coll-Martínez B and Crosas B: How the 26S proteasome degrades ubiquitinated proteins in the cell. biomolecules 9: 395, 2019.
15. Xuan DTM, Wu CC, Kao TJ, Ta HDK, Anuraga G, Andriani V, Athoillah M, Chiao CC, Wu YF, Lee KH, *et al*: Prognostic and immune infiltration signatures of proteasome 26S subunit, non-ATPase (PSMD) family genes in breast cancer patients. Aging (Albany NY) 13: 24882-24913, 2021.
16. Li Y, Liu X, Zhao F, Zhao Z, Li X, Wang J, Huang B and Chen A: Comprehensive analysis of PSMD family members and validation of PSMD9 as a potential therapeutic target in human glioblastoma. CNS Neurosci Ther 30: e14366, 2024.
17. Zhang C, Xu T, Ji K, Cao S, Cao Y, Ai J, Jing L and Sun JH: An integrative analysis reveals the prognostic value and potential functions of PSMD11 in hepatocellular carcinoma. Mol Carcinog 62: 1355-1368, 2023.
18. Huang W, Mei J, Liu YJ, Li JP, Zou X, Qian XP and Zhang Y: An analysis regarding the association between proteasome (PSM) and hepatocellular carcinoma (HCC). J Hepatocell Carcinoma 10: 497-515, 2023.
19. Tsolou A, Nelson G, Trachana V, Chondrogianni N, Saretzki G, von Zglinicki T and Gonos ES: The 19S proteasome subunit Rpn7 stabilizes DNA damage foci upon genotoxic insult. IUBMB Life 64: 432-442, 2012.
20. Livak KJ and Schmittgen TD: Analysis of relative gene expression data using real-time quantitative PCR and the 2-ΔΔCT method. Methods 25: 402-408, 2001.
21. Bray F, Ferlay J, Soerjomataram I, Siegel RL, Torre LA and Jemal A: Global cancer statistics 2018: GLOBOCAN estimates of incidence and mortality worldwide for 36 cancers in 185 countries. CA Cancer J Clin 68: 394-424, 2018.
22. Han B, Zheng R, Zeng H, Wang S, Sun K, Chen R, Li L, Wei W and He J: Cancer incidence and mortality in China, 2022. J Natl Cancer Cent 4: 47-53, 2024.
23. Valery PC, Laversanne M, Clark PJ, Petrick JL, McGlynn KA and Bray F: Projections of primary liver cancer to 2030 in 30 countries worldwide. Hepatology 67: 600-611, 2018.
24. Singal AG, Kanwal F and Llovet JM: Global trends in hepatocellular carcinoma epidemiology: Implications for screening, prevention and therapy. Nat Rev Clin Oncol 20: 864-884, 2023.
25. Zhao K, Zhou X, Xiao Y, Wang Y and Wen L: Research progress in alpha-fetoprotein-induced immunosuppression of liver cancer. Mini Rev Med Chem 22: 2237-2243, 2022.
26. Zhou SS, Ye YP, Chen Y, Zeng DT, Zheng GC, He RQ, Chi BT, Wang L, Lin Q, Su QY, *et al*: Overexpression pattern, function, and clinical value of proteasome 26S subunit non-ATPase 6 in hepatocellular carcinoma. World J Clin Oncol 16: 99839, 2025.
27. Zhou C, Li H, Han X, Pang H, Wu M, Tang Y and Luo X: Prognostic value and molecular mechanisms of proteasome 26S subunit, non-ATPase family genes for pancreatic ductal adenocarcinoma patients after pancreaticoduodenectomy. J Invest Surg 35: 330-346, 2022.
28. Guedes RA, Serra P, Salvador JA and Guedes RC: Computational approaches for the discovery of human proteasome inhibitors: An overview. Molecules 21: 927, 2016.
29. Zong Q, Mao B, Zhang HB, Wang B, Yu WJ, Wang ZW and Wang YF: Comparative Ubiquitome analysis reveals deubiquitinating effects induced by Wolbachia infection in drosophila melanogaster. Int J Mol Sci 23: 9459, 2022.
30. Donne R and Lujambio A: The liver cancer immune microenvironment: Therapeutic implications for hepatocellular carcinoma. Hepatology 77: 1773-1796, 2023.
31. Ruff SM, Shannon AH, Beane JD and Pawlik TM: Highlighting novel targets in immunotherapy for liver cancer. Expert Rev Gastroenterol Hepatol 16: 1029-1041, 2022.